Proteomic Analysis of Soft Tissue Tumor Implants Treated with a Novel Poly*bis*phosphonate

AYODELE ALAIYA[1], JONATHAN FOX[2], STEVE BOBIS[3], GORAN MATIC[3], ZAKIA SHINWARI[1], EMAN BARHOUSH[1], MARCELA MÁRQUEZ[4], STEN NILSSON[4] and ANDERS R. HOLMBERG[4]

[1]*Proteomics Unit, Stem Cell & Tissue Re-Engineering Program, and*
[3]*Department of Comparative Medicine, King Faisal Specialist Hospital and Research Centre, Riyadh, Saudi Arabia;*
[2]*Waters U.K. Limited, Manchester, U.K.;*
[4]*Department of Oncology and Pathology, Karolinska Institute, Stockholm, Sweden*

Abstract. *Background: Osteodex is a novel bi-functional macromolecular polybisphosphonate developed for treatment of bone metastases in prostate and breast cancer. High efficacy of osteodex has been demonstrated both in vitro and in vivo. The present study investigates whether osteodex is also efficacious on soft tissue tumor lesions. Materials and Methods: Twelve female nude mice were injected with MDA-MB-231 cells orthotopically. Osteodex was administered i.v. at 2.5 mg/kg, once per week for five weeks. Tumor volumes were measured during the treatment period, the animals were sacrificed, and samples collected for proteomic analysis. Results: The non-treated mice developed multiple tumors greater than 4 cm with pronounced ulceration, while the treated mice had tumors smaller than 1 cm, without ulceration. While general condition of treated mice was good, non-treated animals were in poor condition. Sixteen out of 300 identified proteins were differentially expressed, with statistically significant expression changes of more than two-fold differences between treated and non-treated groups. These proteins were identified using non-gel based nano-liquid chromatography coupled with a Synapt G2 instrument. Conclusion: We conclude that osteodex showed significant treatment efficacy on soft tissue tumor implants. The study provides a global view of changes in protein expression profiles following osteodex treatment. Some functions of the identified proteins might be used to explain the specific treatment efficacy of osteodex.*

Correspondence to: Dr. Ayodele Alaiya, Proteomics Unit, Stem Cell & Tissue Re-Engineering Program, King Faisal Specialist Hospital and Research Centre, (KFSH&RC) P.O. Box 3354, Riyadh, 11211 Saudi Arabia. Tel: +966 14424718, Fax: +966 14427858, e-mail: AAlaiya@kfshrc.edu.sa

Key Words: Soft tissue, tumor implants, osteodex, proteomic analysis, breast cancer.

Prostate and breast cancer most commonly develop metastases in the skeleton. At an advanced metastatic stage, more than 70% of patients develop bone metastases. Stephen Paget's seed and soil hypothesis, stating that circulating cancer cells can only grow where the microenvironment is permissive for growth, is still appropriate. The continuous re-modeling of bone, involving osteoclasts and osteoblasts, generates the release of multiple cytokines, chemokines and growth factors that are favorable for tumor cell growth (1-3). This, in the presence of a locally rich vasculature and high permeability surrounding of the bone marrow might explain the propensity for bone metastasis in advanced prostate and breast cancer. Even though bone is the most common site of metastasis, soft tissue metastasis often occurs at advanced stage of both prostate and breast cancer. The most common sites are lymphatic nodes, liver and lung (4-9). Lymph nodes close to the primary tumor are often the first sites of tumor spread. In prostate cancer, spinal metastasis often precedes liver and lung metastasis. Approximately half of women with metastatic breast cancer develop liver metastases. In general, detection of positive lymph nodes indicates a poor prognosis and might also be an indicator of an aggressive tumor phenotype. Both advanced prostate and breast cancer are treated with combinations of chemotherapy, radiation, hormonal, and biological therapies (10, 11).

Osteodex is a bi-functional poly*bis*phosphonate recently developed for the treatment of bone metastases. Osteodex is comprised of a carbohydrate polymer with bisphosphonate and guanidine moieties linked to the polymeric backbone. Previous *in vitro* and *in vivo* studies have demonstrated significant bi-functional efficacy *i.e.* inhibition of bone resorption and antitumor efficacy (12, 13). Its mode of action depends on three primary effects: inhibition of the mevalonate pathway, induction of apoptosis, and general cytotoxicity. Clinical phase I study of osteodex was recently completed in patients with castration-resistant prostate cancer (CRPC) and a phase II study is planned for 2014. Osteodex is a macromolecule with certain

electrostatic charge characteristics and, therefore, it seems reasonable that it might also be able to accumulate in breast tumor lesions dependent on the enhanced permeability and retention effect (14).

The present study investigated whether osteodex might have efficacy against soft tissue lesions. Proteomic analysis was the primary method used to investigate the effects on the proteome after osteodex treatment.

Materials and Methods

Osteodex synthesis. Osteodex was prepared as described previously (13). Briefly, Dextran 40 PhEUR (Pharmacosmos AS, Holbaek, Denmark) was oxidized with sodium meta-periodate (Merck AG, Darmstadt, Germany) and amino guanidine and alendronate (Sigma-Aldrich, Stockholm, Sweden) were subsequently conjugated. Sodium borohydride (Chemicon, Stockholm, Sweden) was used for reductive amination. PD-10 disposable Sephadex G-25 columns were used for separation and purification (G&E, Biotech AB, Onsala, Sweden). The conjugation yield was determined by elemental analysis (total nitrogen, total phosphorous; Mikrokemi AB, Uppsala, Sweden).

Animals. Twelve female nude mice (age 6-8 weeks/weighing approximately 18-25 g) were injected with approximately 1-1.5 million MDA-MB-231 cells (Manassas, VA, USA) subcutaneously around the mammary pad region. Tumors developed within 10-14 days post-injection in 9 out of 12 mice and allowed tumor growth to less than 1 cm before initiating treatment with osteodex. The nine tumor-bearing mice were divided into treated (n=5) and no-treatment (n=4) groups.

Thereafter the five tumor-bearing mice were treated with a single dose of osteodex, given intravenously *via* the tail vein at a dose of 2.5 mg/kg, once per week for five weeks. Serial measurements of tumor growth during the period of the experiment were taken until the animals are sacrificed. The measurements were difficult in the non-treated group due to extensive tumor growth with massive ulcerations.

After the treatment period, the animals were sacrificed and gross autopsy was performed. Tumor tissues were resected from both groups for proteomic analysis. All procedures were carried out in strict accordance with an approved protocol for the use of animals in research. The mice were handled and cared for according to Institutional Animal Care and Use Committee (IACUC) policies and guidelines of the office of Research Affairs (RAC# 2080-052), and Animal facility protocol at KFSHRC. The animals were kept in the animal facility at the Comparative Medicine Department and all procedures were performed according to standard guidelines.

Gross autopsy. The abdominal cavity was opened in all animals and gross autopsy was performed. Gross appearances of treated and non-treated animals were recorded including visible extra-abdominal tumors. The peritoneum was inspected, looking for evidence of infiltration and spread in the peritoneal cavity. Histologically-proven representative tissue samples were collected for proteomic analysis. Sample preparation and proteomic analysis. The samples were prepared immediately after the autopsy. Tumor cells were extracted by non-enzymatic method as previously described (15, 16). Briefly, fresh tumor samples were mechanically homogenized in 1-2 ml ice-cold RPMI-1640 medium supplemented with 5% calf serum and protease inhibitors (0.2 mM phenylmethylsulfonyl fluoride (PMSF)/0.83 mM benzamidine). Tissue debris and connective tissues were removed using a 500 μm mesh filter and tumor cells were harvested following percoll centrifugation. The collected cell suspensions were washed twice in phosphate buffered saline containing protease inhibitor cocktails and then centrifuged at 800× *g* and 4˚C for 3 min. Finally, all the samples were centrifuged for 5 min at 2700× *g* (4˚C). The pellets were stored at −80˚C for further analysis.

Protein in-solution digestion and Liquid chromatography–mass spectrometry analysis. The protein concentrations of the whole cell lysates were determined by the Bradford assay method. Protein concentrations of all samples were normalized and for each sample, 100 μg complex protein mixture was taken and exchanged twice with 500 μl of 0.1% RapiGest (Waters, Manchester, UK) (1 vial diluted in 1,000 μl 50 mM AmBic) with a 3-kDa ultra filtration device (Millipore, Bedford, MA, USA). Protein concentration of between 0.1 and 1 μg/μl was achieved at the end of digestion. Proteins were denatured in 0.1% RapiGest SF at 80˚C for 15 min, reduced in 10 mM Dithiothreitol at 60˚C for 30 min, spinned down and allowed to cool to room temperature and alkylated in 10 mM iodoacetamide for 40 min at room temperature in the dark. Samples were trypsin-digested at a 1:50 (w/w; 1 μg/μl trypsin concentration) enzyme:protein ratio and trypsin, for at least 4 h or overnight at 37˚C with gentle shaking. The digestion was ended and RapiGest quenched with 4 μl of 12 M HCl at 37˚C for 15 min and centrifuged at 17,900 RCF for 10 min. Samples were diluted to 5 pmol/μl or 5- to 10-fold with aqueous 0.1% formic acid prior to LC/MS analysis. All samples were spiked with yeast alcohol dehydrogenase (ADH; P00330) as internal standard to the digests to give 200 fmol per injection for absolute quantitation.

Protein identification by mass spectrometry-LC/MS^E. Both qualitative and quantitative expression profiling were performed using 1-dimensional Nano Acquity liquid chromatography coupled with tandem mass spectrometry on a Synapt G2 instrument (Waters Scientific, Berkshire, UK). The instrument settings for Electrospray Ionization Mass Spectrometry analyses were optimized on the tune page as follows: Detectors set up using 2 ng/μl leucine enkephalin (556.277 Da), Mass (*m/z*) calibration was achieved on a separate infusion of 500 fmol [Glu] 1-fibrinopeptide B (GluFib, 785.843 Da), using the Mass Lynx IntelliStart. Other parameters included capillary voltage 3 kV,, sample cone 50 V, extraction cone 5 V, source temperature 80˚C, cone gas 10 l/h, nano flow gas 0.5 bar and purge gas 800 l/h. All analyses were carried out on Trizaic Nano source (Waters) ionization in the positive ion mode nanoESI.

A total of 2 μg protein digest was loaded on column and samples were processed using the Acquity sample manager with mobile phase consisting of A1 (water + 0.1% formic acid) and B1 (acetonitrile + 0.1% formic acid) with sample flow rate of 0.500 μl/min. Data-independent acquisition (MS^E)/iron mobility separation experiments were performed and data was acquired over a range of *m/z* 50-2000 Da with a scan time of 1 s, ramped transfer collision energy 20-50 V with a total acquisition time of 120 min. All samples were analyzed in triplicate runs and data were acquired using the Mass Lynx programs (version. 4.1, SCN833; Waters) operated in resolution and positive polarity modes. The acquired MS data were background-subtracted, smoothed and de-isotoped at medium threshold. Protein Lynx Global Server (PLGS) 2.2 (Waters) was used for all automated data processing and database searching. The generated peptide masses were searched against Uniprot protein sequence database using the PLGS 2.2 for protein identification (Waters).

Table I. *A summary of clinical and histopathological findings. Rx: Osteodex-treated; No RX: non-treated mice.*

Sample #	Tissue	Pathology extent of tumor/necrosis	Physical status
Rx1 1986	Liver	No tumor	Active, eating well, tumor shape well-defined, good skin coloration, no ulceration
	Kidney	Multiple foci of cancer	
	Tumor	Carcinoma	
Rx2 1981	Liver	No tumor	Active, eating well, tumor shape well defined, good skin coloration, no ulceration
	Kidney	Foci of cancer	
	Tumor	Carcinoma	
Rx3 1978	Liver	No tumor	Active, eating well, tumor shape well defined, good skin coloration, no ulceration
	Kidney	Foci of viable cancer	
	Tumor	Carcinoma + 100% necrosis	
Rx4 1985	Liver	No tumor	Active, eating well, tumor shape well defined, good skin coloration, no ulceration
	Kidney	Few tumor cells	
	Tumor	Carcinoma	
Rx5 1984	Liver	No tumor	Very active, eating well, tumor shape well defined, good skin coloration, no ulceration
	Kidney	No cancer cells seen	
	Tumor	Carcinoma	
No Rx1 _1979	Liver	No tumor	Less active, not eating well, tumor shape diffused, massive sub cutaneous vascularization around tumor, tumor ulceration
	Kidney	Extensive tumor involvement	
	Tumor	Carcinoma + 50% necrosis	
No Rx2 _1980	Liver	Foci of cancer	(Died) Less active, not eating well, tumor shape diffused, massive sub cutaneous vascularization around tumor, tumor ulceration
	Kidney	metastatic cancer	
	Tumor	Massive ulcerative tumor	
No Rx3 _1991	Liver	No tumor	Less active, not eating well, tumor shape diffused, massive sub cutaneous vascularization around tumor, tumor ulceration
	Kidney	Extensive tumor + vascular invasion	
	Tumor	Carcinoma	
No Rx4 _1992	Liver	Multiple foci of cancer	Sacrificed earlier due to reduced physical activity, not eating well, tumor shape diffused, massive sub cutaneous vascularization around tumor, tumor ulcerations
	Kidney	Extensive metastatic cancer	
	Tumor	Massive ulcerative carcinoma	

Data analysis and informatics. TransOmics Informatics (Waters) was used to process and search the data. A human database containing 46,906 reviewed entries was downloaded from Uniprot. A decoy database was created by reversing this and concatenated to the original database prior to searching. The principle of the search algorithm is described by Li *et al*. (17). The following criteria were used for the search: one missed cleavage, maximum protein mass 1000 kDa, trypsin, carbamidomethyl C fixed and oxidation M variable modifications.

Normalized label-free quantification was achieved using exclusive TransOmics software, developed in collaboration with Nonlinear Dynamics (Newcastle, UK), and was used to plot Principal component analysis (PCA) analysis against data split into two groups. The data were filtered to show only statistically (ANOVA) significantly altered proteins ($p \leq 0.05$) with ≥3 peptides identified and a fold change of more than 2.

Additionally 'Hi3' absolute quantification was performed using ADH as an internal standard to give an absolute amount of each identified protein (Waters).

Results

Before sacrificing the animals for autopsy, it was noted that treated animals were in good and normal condition while non-treated animals were doing poorly due to extensive disease progression. Serial measurements of tumor growth/volume revealed a statistically significant difference between treated and non-treated animals (Figure 1A). Osteodex-treated animals had small well-demarcated lesions while non-treated animals presented with large infiltrating and ulcerating lesions (Figure 1B).

Gross autopsy. Non-treated animals developed multiple metastatic tumors in the peritoneal cavity, distant metastasis to the kidneys and livers with ulcerations and blood vessel infiltration. Treated animals had a few solitary small lesions in the kidneys but with no further infiltrations in the peritoneal cavity and no metastasis to the liver (Table I). Figure 2 shows representative histological slides by light microscopy of normal kidney glomeruli in a treated animal compared with histological appearance of neoplastic cell infiltrations of the entire kidney of non-treated animals.

To gain insight into the biological changes behind this massive difference in tumor growth, tumor samples from five treated and four non-treated mice were subjected to proteomic comparison.

Proteomic analysis and changes in protein expression. A label-free MS-based method as a tool for comparative

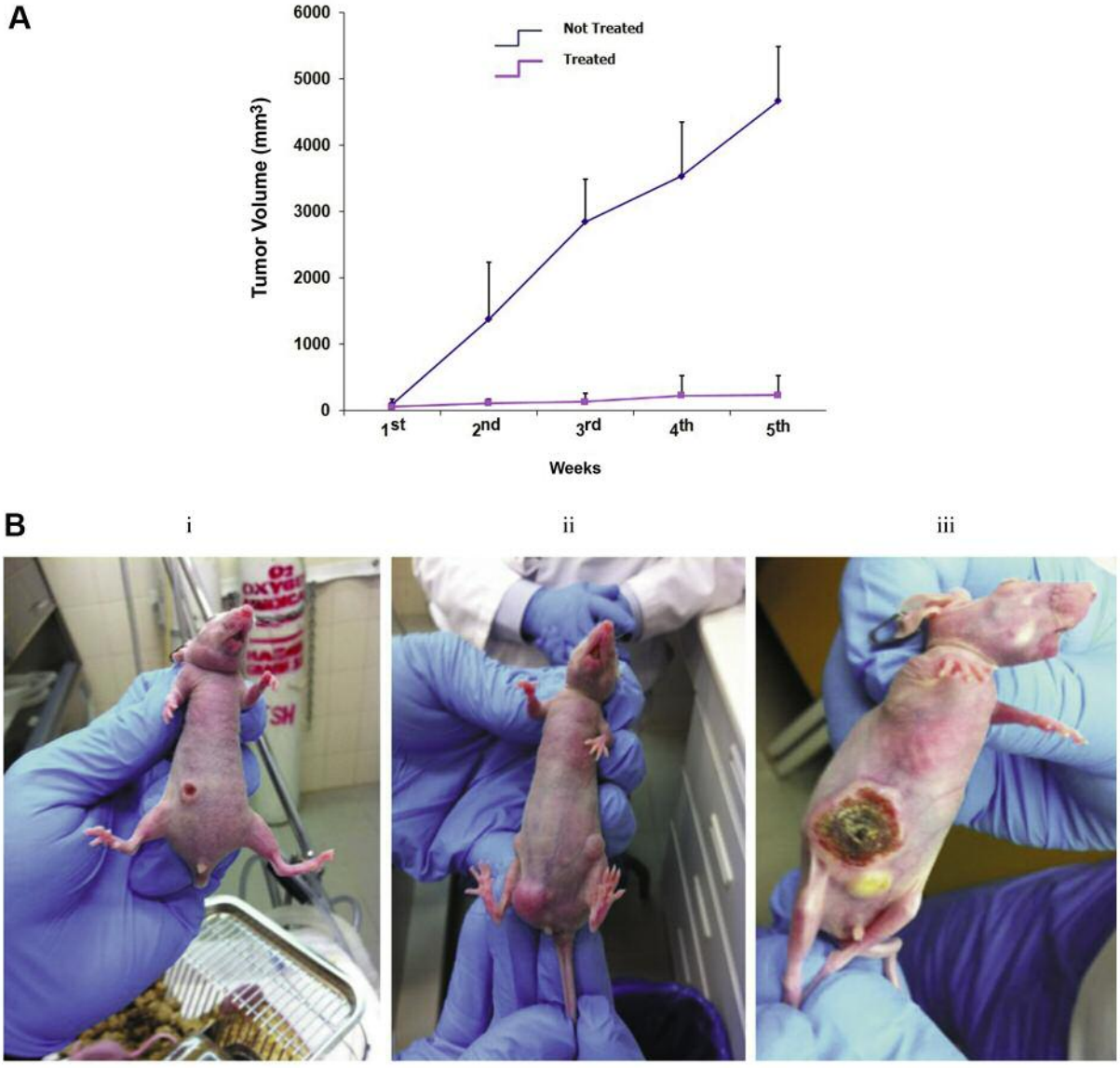

Figure 1. *A: Graph of serial measurements of tumor volume (mm^3) over treatment duration between tumor-bearing treated and non-treated mice (tumor volume V=1/2(width^2×length). B: Photographs showing marked pathological changes (i) very small tumors in the treated group compared with (ii) and (iii) massive and ulcerative tumor in the no treatment group. (Additionally, the mice in the treatment group are much more physically active compared to non-treated mice).*

protein expression profiling was used. A total of 19,420 unique peptide features were detected, filtered outside an area of 50-2000 *m/z* and background noise, and reduced to 11,045. Screening for features that differed significantly between treated and non-treated ($p<0.05$ and $p<0.001$) mice revealed 2,058 features with ~3% false discovery rate (a statistical analysis method used for correction of multiple comparisons, adjusting observed *p*-values to avoid 'over-interpretation' of the significance of the observed results).

The majority of the proteins in the treated group were up-regulated, while the non-treated group had only a very small fraction of these up-regulated. These findings are similar to what was observed with PCA plot generated from 2-DE dataset (data not shown).

Differentially expressed proteins. Approximately 300 proteins from tumor tissues of treated and non-treated mice were identified. Sixteen of these proteins were differentially

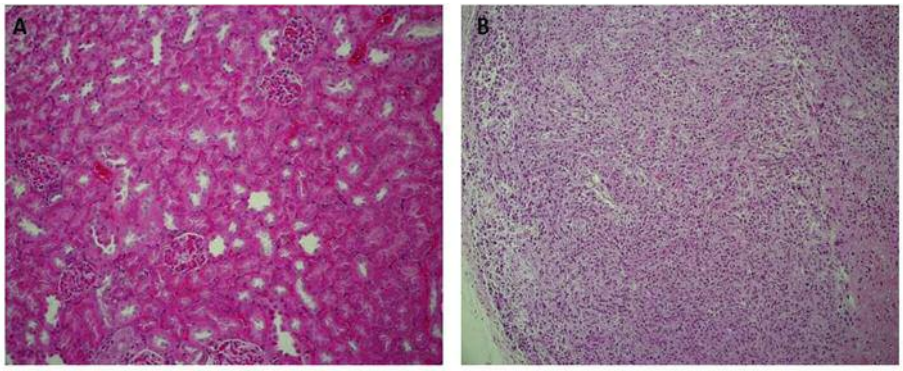

Figure 2. *Representative histological slide by light microscopy of normal kidney glomeruli in a treated tumor-bearing mouse (A) compared to the histological appearance of neoplastic cell infiltration of the entire kidney of a tumor-bearing non-treated mouse (B).*

expressed with significant expression changes of at least two-fold between sample groups (Table II). A data set of the 16 proteins differentially expressed between treatment sample groups clearly discriminated the samples into two distinct groups by unsupervised hierarchical cluster analysis and PCA (Figure 3A and B).

Functional interpretation of the identified proteins. Further characterization of the identified proteins was explored using Ingenuity Pathway Analysis (Ingenuity Systems, Inc., Redwood, CA, USA). The 16 identified proteins were mapped and represented in three sub-signaling networks. Ten proteins were implicated in the network of humoral immune response, inflammatory response and cellular movement, while three of the molecules were involved in networks of molecular transport, hematological system development and function, hematological disease. Only one molecule (type VI protein-arginine deiminase, a member of peptidyl arginine deiminase family) is implicated in the network of cell cycle, cell death and survival, endocrine system disorders (Figure 4).

The summarized functional characteristics of some of the identified proteins are listed in Table III, derived from the Ingenuity Database program. The majority of these molecules are located in the cytoplasm and only a few are located in the extracellular space. While many of them act as enzymes, others act as cellular transporters. Ten proteins were up-regulated, while only four proteins were down-regulated between treated and non-treated groups. Furthermore, four proteins (Hemoglobin, beta adult minor chain (Hbb-b2), Hemoglobin, zeta (HBZ), ATPase, Ca^{++} transporting, cardiac muscle, fast twitch 1 (ATP2A1), and Complement component 3 (C3) were not directly mapped in a network, but were functionally-implicated in cell death and survival in apoptosis of acinar gland cells, as well as in apoptosis of liver cell lines.

Discussion

The present study investigated the efficacy of osteodex treatment on tumor implants in mice and the effects on the tumor cell proteome was examined.

Previous experience from a wide range of chemotherapeutic drugs and other anticancer agents indicate that many result in induction of apoptosis of the malignant cells. Sequences of events occur as tumor cells undergo apoptosis, including DNA and protein degradation. Recently, Ueno *et al*. demonstrated that apoptosis of breast cancer tumor cells can create products detectable in serum (18). Because of laws regulating the patient's integrity, ethical issues *etc*. (Bio bank law Regulations), it is difficult to obtain pre- and post-therapy sequential biopsy samples. Consequently, knowledge and characteristics of apoptotic changes following treatment of solid tumors in humans are limited.

Clinical diagnosis of most malignancies can be made with accuracy, however prediction of treatment response is more difficult and limited. Therefore, there is a considerable need for the discovery and development of sensitive and specific biomarkers for disease prognosis and prediction of treatment response.

Protein biomarkers are often defined as specific proteins that can be quantitatively measured and evaluated as objective indicators of normal state, pathological state, and as an indicator of therapeutic response.

Recent advancements in proteomic analysis technologies have generated further interest in possibilities of translational research. Expression proteomics, often defined as large-scale differential protein profiling analyses, have resulted in identification of disease-related or tissue-specific proteins that could be potentially used as disease biomarkers (19, 20).

Classical expression-based proteomics strategies, including high-resolution two-dimensional protein separations (2-DE)

Table II. *Identified proteins with a significant change in expression (≥2-fold up or down and p-value of 0.001) between ODX treated and no-treatment tumors. (The proteins were identified by LC/MS/MS/Synapt G2.*

Accession	Peptide Counts	Peptides Used for Quanti-fication	Anova (p)	Max fold change	Highest Mean Condition	Lowest Mean Condition	Description	ODXNo-Rx-1 Normalized abundance No RX	ODX_Rx-1 Normalized abundance RX
Q8VCM7	15	12	5.36E-05	2.571180393	No RX	RX	Fibrinogen gamma chain OS=Mus musculus GN=Fgg PE=2 SV=1	48481.01643	18855.5484
Q8K0E8	21	21	0.000382952	2.394511282	No RX	RX	Fibrinogen beta chain OS=Mus musculus GN=Fgb PE=2 SV=1	89515.52179	37383.6292
P58774	8	2	0.000477255	6.5110559	RX	No RX	Tropomyosin beta chain OS=Mus musculus GN=Tpm2 PE=1 SV=1	1223.098675	7963.66384
P56757	2	2	0.000623897	8.409113614	No RX	RX	ATP synthase subunit alpha, chloroplastic OS=Arabidopsis thaliana GN=atpA PE=1 SV=1	1810.524096	215.304987
P16015	2	2	0.000863602	5.18135238	RX	No RX	Carbonic anhydrase 3 OS=Mus musculus GN=Ca3 PE=1 SV=3	593.2642629	3073.9112
Q8CGP6	16	4	0.001673002	2.204667019	No RX	RX	Histone H2A type 1-H OS=Mus musculus GN=Hist1h2ah PE=1 SV=3	17791.04608	8069.72025
Q60605	8	7	0.002061526	3.219196447	RX	No RX	Myosin light polypeptide 6 OS=Mus musculus GN=Myl6 PE=1 SV=3	6465.228067	20812.8392
P16254	1	1	0.002929153	2.264303835	No RX	RX	Signal recognition particle 14 kDa protein OS=Mus musculus GN=Srp14 PE=1 SV=1	3261.017145	1440.18532
P16858	12	8	0.003038352	3.237616414	No RX	RX	Glyceraldehyde-3-phosphate dehydrogenase OS=Mus musculus GN=Gapdh PE=1 SV=2	117269.6565	36220.9853
P06467	3	2	0.004397509	2.005960029	RX	No RX	Hemoglobin subunit zeta OS=Mus musculus GN=Hbz PE=2 SV=2	937.2448276	1880.07566
Q8K3V4	2	2	0.004581663	∞	No RX	RX	Protein-arginine deiminase type-6 OS=Mus musculus GN=Padi6 PE=1 SV=2	457.8284457	0
Q9LKR3	4	1	0.006653714	109.5788538	RX	No RX	Mediator of RNA polymerase II transcription subunit 37a OS=Arabidopsis thaliana GN=MED37A PE=1 SV=1	3.92806052	430.43237
Q8R429	2	2	0.009055467	2.345515462	RX	No RX	Sarcoplasmic/endoplasmic reticulum calcium ATPase 1 OS=Mus musculus GN=Atp2a1 PE=2 SV=1	4051.359374	9502.52606
Q3TYV2	2	1	0.009738446	2.026515784	No RX	RX	HERV-H LTR-associating protein 1 homolog OS=Mus musculus GN=Hhla1 PE=2 SV=1	1682.60173	830.292931
Q5SX40	22	4	0.009991226	3.262071345	RX	No RX	Myosin-1 OS=Mus musculus GN=Myh1 PE=1 SV=1	3859.49146	12589.9365
P99027	2	2	0.013331273	4.253234491	No RX	RX	60S acidic ribosomal protein P2 OS=Mus musculus GN=Rplp2 PE=1 SV=3	2883.427776	677.937645
Q9SF91	2	1	0.013449852	5.324344132	No RX	RX	Ras-related protein RABE1e OS=Arabidopsis thaliana GN=RABE1E PE=1 SV=1	1602.742872	301.021653
P01027	2	2	0.016096267	7.070429139	No RX	RX	Complement C3 OS=Mus musculus GN=C3 PE=1 SV=3	587.1879399	83.0484159
P02089	8	2	0.021295889	5.870299765	RX	No RX	Hemoglobin subunit beta-2 OS=Mus musculus GN=Hbb-b2 PE=1 SV=2	1166.917163	6850.15355
Q922F4	13	2	0.029342032	2.336863076	No RX	RX	Tubulin beta-6 chain OS=Mus musculus GN=Tubb6 PE=1 SV=1	1705.856405	729.977046

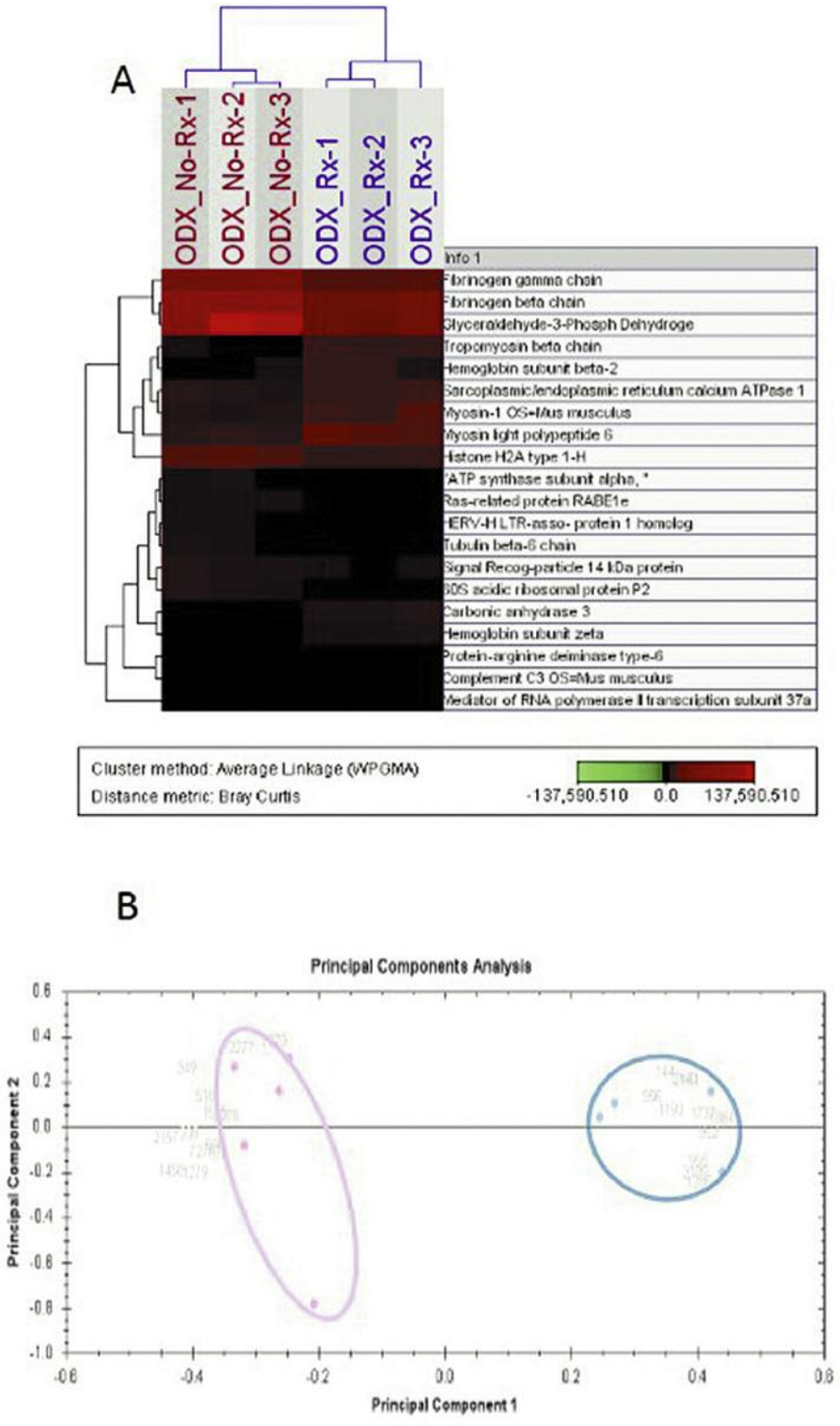

Figure 3. *A: Hierarchical cluster analysis using the 16 identified proteins with significant difference in expression between tumors from osteodex-treated and non-treated mice. The names of the identified proteins are indicated in the dendrogram (red, tumors with no treatment; and blue, osteodex-treated tumors). The dendrogram was generated using the Bray Curtis distance metric and an average linkage clustering method from the J-Express software. B: The same dataset was subjected to principal component analysis (PCA) and the expression changes allow for clear separation into two distinct groups.*

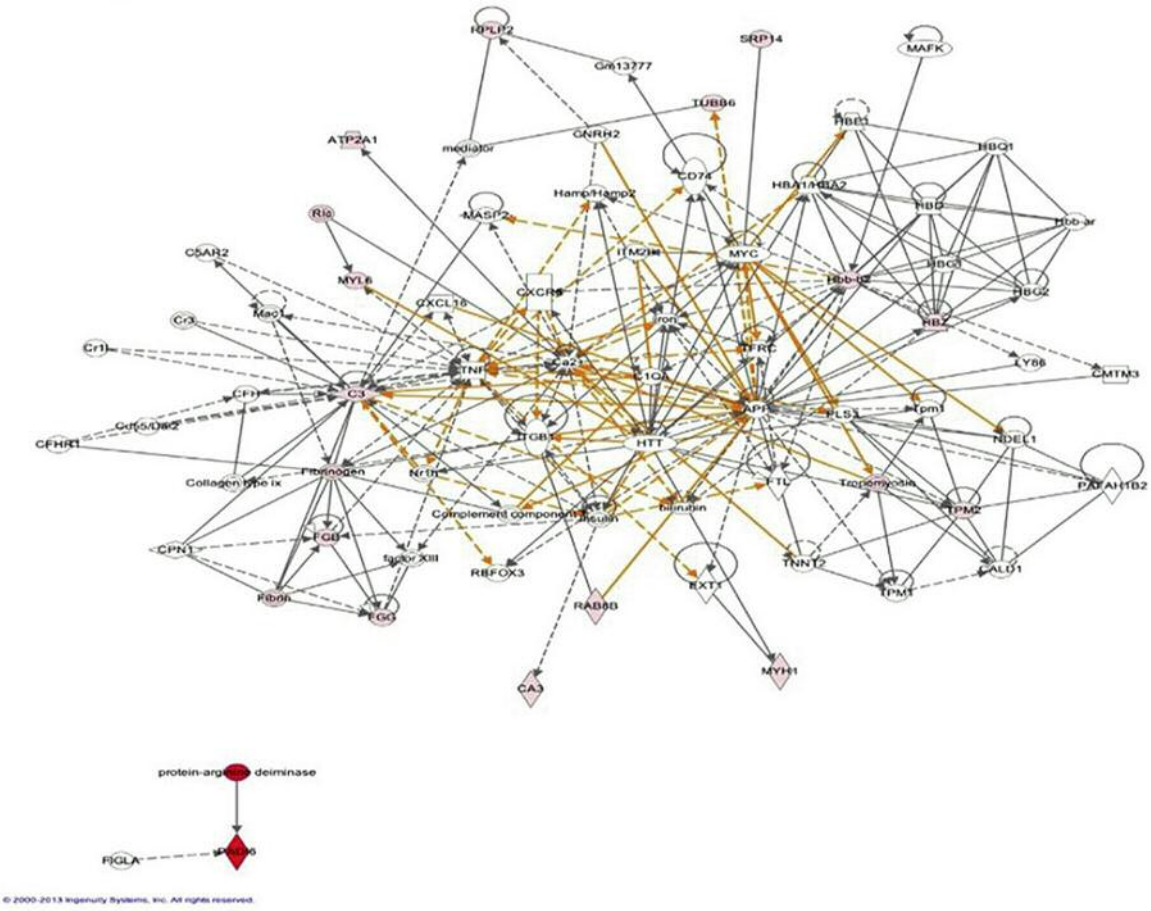

Figure 4. *The 16 identified proteins were mapped and represented in three merged sub-signaling networks. Ten proteins were implicated in the network of humoral immune response, inflammatory response, cellular movement, while three of the molecules were involved in network of molecular transport, hematological system development and function, hematological disease. Only one molecule (type VI protein arginine deiminase, a member of the peptidyl arginine deiminase family) is implicated in the network comprising of cell cycle, cell death and survival, endocrine system disorders. The summarized functional characteristics of some of the identified proteins are listed in Table I. The data were partly obtained using the Ingenuity Database program.*

coupled to highly sensitive protein identification by LC-MS-MS, can identify novel protein markers. Large amounts of differential expression data can be analyzed by artificial learning methods, yielding disease diagnosis or monitoring treatment response.

In the present study, we used hierarchical cluster analysis of qualitative and quantitative in-solution protein expression changes in an attempt to monitor and interpret changes as a result of osteodex therapy on breast tumors. Using protein expression changes coupled to protein identification by tandem mass spectrometry, 16 differentially expressed proteins associated with osteodex treatment were found. The expression of these proteins clearly discriminates between treated and non-treated groups (Figure 3 A and B). The majority of proteins in the treatment group were distinctly up-regulated in contrast to those in the non-treated group, indicating altered protein expression associated with the osteodex treatment. The proteins' functional characteristics were established using the ingenuity pathway analysis. Fifteen out of the 16 identified proteins were associated with different signaling networks, including humoral immune response, inflammatory response, cellular movement, molecular transport, hematological system development and function, hematological disease. One of the 16 proteins, absent in the treatment group and only expressed in the non-treated group, was an enzyme, type-6 protein-arginine deiminase (PAD), a member of peptidyl arginine deiminase family, associated with the network affecting cell cycle, cell death and survival. PAD belongs to a group of enzymes involved in post-translational protein de-aminations. They act as catalysts in the conversion of arginine residues into citrullines by the addition of calcium ions. PAD1, -2, -3 and -4 have so far been described in human

Table III. *Functional annotation of some of the identified proteins with expressively significant change (≥2-fold up or down and p-value of 0.001) between osteodex-treated and no treatment tumors. The proteins were identified by an LC-MS/MS Synapt G2.*

Fold Change	ID	Symbol	Entrez Gene Name	Location	Type(s)
2.346	Q8R429	ATP2A1	ATPase, Ca++ transporting, cardiac muscle, fast twitch 1	Cytoplasm	Transporter
7.070	P01027	C3	Complement component 3	Extracellular Space	Peptidase
5.181	P16015	*CA3	Carbonic anhydrase III, muscle specific	Cytoplasm	Enzyme
2.395	Q8K0E8	FGB	Fibrinogen beta chain	Extracellular Space	Other
2.571	Q8VCM7	FGG	Fibrinogen gamma chain	Extracellular Space	Other
5.870	P02089	Hbb-b2	Hemoglobin, beta adult minor chain	Unknown	Other
2.006	P06467	HBZ	Hemoglobin, zeta	Cytoplasm	Transporter
2.027	Q3TYV2	HHLA1	HERV-H LTR-associating 1	Unknown	Other
3.262	Q5SX40	MYH1	Myosin, heavy chain 1, skeletal muscle, adult	Plasma Membrane	Enzyme
3.219	Q60605	MYL6	Myosin, light chain 6, alkali, smooth muscle and non-muscle	Cytoplasm	Other
∞.000	Q8K3V4	PADI6	Peptidyl arginine deiminase, type VI	Cytoplasm	Enzyme
5.324	Q9SF91	RAB8B	RAB8B, member RAS oncogene family	Cytoplasm	Enzyme
4.253	P99027	RPLP2	Ribosomal protein, large, P2	Cytoplasm	Other
2.264	P16254	SRP14	Signal recognition particle 14kDa (homologous Alu RNA binding protein)	Cytoplasm	Other
6.511	P58774	TPM2	Tropomyosin 2 (beta)	Cytoplasm	Other
2.337	Q922F4	$**TUBB6	Tubulin, beta 6 class V	Cytoplasm	Other

*Implicated in Carbonic anhydrase inhibitor agents, in osteoporosis; $Implicated in an antibody-drug conjugate (brentuximab vedotin) approved to treat anaplastic large cell lymphoma (ALCL); **Implicated in a semi-synthetic derivative of a natural taxoid (cabazitaxel), recently FDA approved for the treatment of hormone-refractory prostate cancer. The table was partly generated from Ingenuity Systems, Inc. All rights reserved 2000-2013.

genes and their expressions cut across a wide variety of tissues and are thought to play a role in the onset and progression of human neurodegenerative disorders such as Alzheimer's disease and multiple sclerosis. PAD6 has not been well-characterized in human tumors (21). The observation of its high expression in the non-treated group and absence in treated tumor is interesting and might indicate a potential marker for monitoring osteodex treatment response.

Tubulin β6 class V, a cytoplasmic protein, was significantly down-regulated in the samples from osteodex-treated mice. Tubulins belong to a superfamily of cytoplasmic proteins. Six members have been characterized, the α-, β-, γ-, δ-, ε- and the ζ-tubulin. α-Tubulin and β-tubulin are associated with the cellular dynamic/stability of microtubules and are prevalent members of the tubulin family. Many anticancer agents have β-tubulin binding activity, resulting in microtubule re-arrangements and ultimately cell-cycle blockage. The expression pattern of different tubulins after anticancer treatment has been investigated to elucidate their possible usefulness as markers for treatment outcome. In general, the global expression of the different β-tubulin isotypes showed varied and complex patterns across different tumor types (22).

A recent colorectal cancer study demonstrated a link between poor survival and the expression of Tubulin, beta 3 (TUBB3)/TUBB6, and the androgen receptor (AR), especially in females. In both genders, AR is associated with TUBB3/TUBB6 expression (23).

The semi-synthetic taxane derivative cabazitaxel works by disruption of the microtubular network necessary for cellular functions, especially during mitotic and interphase of cell division. This compound was recently approved by the Food and Drug Administration (FDA) for treatment of CRPC. With this perspective regarding the importance of effects on tubulins, the observation in this study is interesting and significant. Tubulin markers once validated might become useful in the monitoring of response to treatment of patients with CRPC.

Three proteins with the most marked difference in samples between non-treated and osteodex-treated mice were fibrinogen gamma and beta chains, Myosin light polypeptide 6 and glyceraldehyde-3-phosphate dehydrogenase (GAPDH). The highest mean expression of myosin light polypeptide 6 was observed among the samples from treated mice, while the other three proteins were significantly highly expressed in the samples from non-treated tumors. Of particular interest a greater than three-fold inverse expression of GAPDH in the treatment group was observed. This 38-kDa protein is an important catalytic enzyme necessary for ATP production in cells. It was recently demonstrated that GAPDH is regulated to target telomerase architecture, resulting in an arrest of telomere maintenance, induction of cancer cell senescence and increased cancer cell proliferation (24). Therefore, the present results suggest that treatment with osteodex inhibits GAPDH expression, thereby resulting in inhibition of tumor growth.

Cytoskeletal proteins are actively involved in regulation of cellular structure and the ability of the cells to maintain structural integrity is a fundamental aspect of cellular responses to injury or therapeutic agents. A recent study demonstrated that myosin light chain kinase significantly enhanced the highly proliferative ability of breast cancer cells mediated by anti-apoptosis linked to the p38 pathway (25). The enhanced cell proliferation of the samples from the non-treated group, with highly up-regulated expression of myosin light polypeptide 6 and the marked expression reduction in samples from osteodex-treated animals are another interesting observation indicating the efficacy of osteodex.

In summary, the present study indicates that osteodex, although bone-specific, exerts a considerable efficacy on soft tissue lesions also. Several of the differentially expressed protein patterns indicate a broad and significant mode of action. Some of these might have the potential to serve as markers of therapeutic response.

The present study further demonstrates the versatility of proteomic analyses and its constantly evolving technical advancement.

Disclosure and Conflict of Interest

None.

Acknowledgements

The Authors wish to acknowledge the support of the Research Center Administration at the King Faisal Specialist Hospital & Research Center. We are thankful for the support and logistic assistance from Logistics and Facilities Management Office. This work was supported by King Faisal Specialist Hospital and Research Centre (RAC Project # 2080 052). We thankfully acknowledge Mr. Abdallah Al-Dhfyan for technical assistance. This study was supported by The Cancer Society in Stockholm, The King Gustav V Jubilee Fund, Stockholm, The Swedish Cancer Society, and Mr Svante Wadman, Stockholm.

References

1 Buijs JT and van der Pluijm G: Osteotropic cancers: from primary tumor to bone. Cancer letters *273*: 177-193, 2009.

2 Bussard KM, Gay CV, and Mastro AM: The bone microenvironment in metastasis; what is special about bone? Cancer metastasis reviews *27*: 41-55, 2008.

3 Paget S: The distribution of secondary growths in cancer of the breast. 1889. Cancer metastasis reviews *8*: 98-101, 1989.

4 Bubendorf L, Schopfer A, Wagner U, Sauter G, Moch H, Willi N, Gasser TC and Mihatsch MJ: Metastatic patterns of prostate cancer: an autopsy study of 1,589 patients. Human pathology *31*: 578-583, 2000.

5 Datta K, Muders M, Zhang H and Tindall DJ: Mechanism of lymph node metastasis in prostate cancer. Future oncology *6*: 823-836, 2010.

6 Elias D and Di Pietroantonio D: Surgery for liver metastases from breast cancer. HPB: the official journal of the International Hepato Pancreato Biliary Association *8*: 97-99, 2006.

7 Jatoi I, Hilsenbeck SG, Clark GM and Osborne CK: Significance of axillary lymph node metastasis in primary breast cancer. Journal of clinical oncology: official journal of the American Society of Clinical Oncology *17*: 2334-2340, 1999.

8 Long MA and Husband JE: Features of unusual metastases from prostate cancer. The British journal of radiology *72*: 933-941, 1999.

9 Roche H and Vahdat LT: Treatment of metastatic breast cancer: second line and beyond. Annals of oncology: official journal of the European Society for Medical Oncology/ESMO *22*: 1000-1010, 2011.

10 Tkaczuk KH: Review of the contemporary cytotoxic and biologic combinations available for the treatment of metastatic breast cancer. Clinical therapeutics 31 Pt *2*: 2273-2289, 2009.

11 Tran C, Ouk S, Clegg NJ, Chen Y, Watson PA, Arora V, Wongvipat J, Smith-Jones PM, Yoo D, Kwon A, Wasielewska T, Welsbie D, Chen CD, Higano CS, Beer TM, Hung DT, Scher HI, Jung ME, and Sawyers CL: Development of a second-generation antiandrogen for treatment of advanced prostate cancer. Science *324*: 787-790, 2009.

12 Daubine F, R LEB, Marquez M, Nilsson S, Schroder T and Holmberg AR: Treatment of bone metastasis in prostate cancer: efficacy of a novel polybisphosphonate. Anticancer Res *31*: 4141-4145, 2011.

13 Holmberg AR, Lerner UH, Alayia AA, Al-Mohanna M, Adra C, Marquez M, Meurling L and Nilsson S: Development of a novel poly bisphosphonate conjugate for treatment of skeletal metastasis and osteoporosis. International journal of oncology *37*: 563-567, 2010.

14 Greish K: Enhanced permeability and retention (EPR) effect for anticancer nanomedicine drug targeting. Methods in molecular biology *624*: 25-37, 2010.

15 Alaiya AA, Franzen B, Moberger B, Silfversward C, Linder S and Auer G: Two-dimensional gel analysis of protein expression in ovarian tumors shows a low degree of intratumoral heterogeneity. Electrophoresis *20*: 1039-1046, 1999.

16 Franzen B, Auer G, Alaiya AA, Eriksson E, Uryu K, Hirano T, Okuzawa K, Kato H and Linder S: Assessment of homogeneity in polypeptide expression in breast carcinomas shows widely variable expression in highly malignant tumors. International journal of cancer Journal international du cancer *69*: 408-414, 1996.

17 Li GZ, Vissers JP, Silva JC, Golick D, Gorenstein MV and Geromanos SJ: Database searching and accounting of multiplexed precursor and product ion spectra from the data independent analysis of simple and complex peptide mixtures. Proteomics *9*: 1696-1719, 2009.

18 Ueno T, Toi M, and Linder S: Detection of epithelial cell death in the body by cytokeratin 18 measurement. Biomedicine & pharmacotherapy=Biomedecine & pharmacotherapie 59 Suppl *2*: S359-362, 2005.

19 Alaiya A, Al-Mohanna M, and Linder S: Clinical cancer proteomics: promises and pitfalls. Journal of proteome research *4*: 1213-1222, 2005.

20 Linder S and Alaiya A: Serum efficacy biomarkers for oncology. Biomarkers in medicine *3*: 47-54, 2009.

21 Chavanas S, Mechin MC, Takahara H, Kawada A, Nachat R, Serre G and Simon M: Comparative analysis of the mouse and

human peptidylarginine deiminase gene clusters reveals highly conserved non-coding segments and a new human gene, PADI6. Gene *330*: 19-27, 2004.

22 Leandro-Garcia LJ, Leskela S, Landa I, Montero-Conde C, Lopez-Jimenez E, Leton R, Cascon A, Robledo M and Rodriguez-Antona C: Tumoral and tissue-specific expression of the major human beta-tubulin isotypes. Cytoskeleton *67*: 214-223, 2010.

23 Mariani M, Zannoni GF, Sioletic S, Sieber S, Martino C, Martinelli E, Coco C, Scambia G, Shahabi S and Ferlini C: Gender influences the class III and V beta-tubulin ability to predict poor outcome in colorectal cancer. Clinical cancer research : an official journal of the American Association for Cancer Research *18*: 2964-2975, 2012.

24 Nicholls C, Pinto AR, Li H, Li L, Wang L, Simpson R and Liu JP: Glyceraldehyde-3-phosphate dehydrogenase (GAPDH) induces cancer cell senescence by interacting with telomerase RNA component. Proceedings of the National Academy of Sciences of the United States of America *109*: 13308-13313, 2012.

25 Cui WJ, Liu Y, Zhou XL, Wang FZ, Zhang XD and Ye LH: Myosin light chain kinase is responsible for high proliferative ability of breast cancer cells *via* anti-apoptosis involving p38 pathway. Acta pharmacologica Sinica *31*: 725-732, 2010.

Received January 17, 2014
Revised January 30, 2014
Accepted January 31, 2014